

Genetic Basis of Evolutionary Adaptation by *Escherichia coli* to Stressful Cycles of Freezing, Thawing and Growth

Sean C. Sleight,^{*,1} Christian Orlic,^{*} Dominique Schneider^{†,‡} and Richard E. Lenski^{*}

^{*}Department of Microbiology and Molecular Genetics, Michigan State University, East Lansing, Michigan 48824,

[†]Laboratoire Adaptation et Pathogénie des Micro-organismes, Université Joseph Fourier Grenoble 1, F-38042

Grenoble Cedex 9, France and [‡]CNRS UMR 5163, F-38042 Grenoble Cedex 9, France

Manuscript received May 12, 2008

Accepted for publication July 7, 2008

ABSTRACT

Microbial evolution experiments offer a powerful approach for coupling changes in complex phenotypes, including fitness and its components, with specific mutations. Here we investigate mutations substituted in 15 lines of *Escherichia coli* that evolved for 1000 generations under freeze–thaw–growth (FTG) conditions. To investigate the genetic basis of their improvements, we screened many of the lines for mutations involving insertion sequence (IS) elements and identified two genes where multiple lines had similar mutations. Three lines had IS150 insertions in *cls*, which encodes cardiolipin synthase, and 8 lines had IS150 insertions in the *uspA-uspB* intergenic region, encoding two universal stress proteins. Another line had an 11-bp deletion mutation in the *cls* gene. Strain reconstructions and competitions demonstrated that this deletion is beneficial under the FTG regime in its evolved genetic background. Further experiments showed that this *cls* mutation helps maintain membrane fluidity after freezing and thawing and improves freeze–thaw (FT) survival. Reconstruction of isogenic strains also showed that the IS150 insertions in *uspA/B* are beneficial under the FTG regime. The evolved insertions reduce *uspB* transcription and increase both FT survival and recovery, but the physiological mechanism for this fitness improvement remains unknown.

EVOLUTIONARY biologists have long been interested in elucidating the genetic bases of adaptation to particular environments, including especially those environments that are novel or stressful to the organism. Evolution experiments using bacteria and other microorganisms (ELENA and LENSKI 2003; POON and CHAO 2005; RIEHLE *et al.* 2005; HERRING *et al.* 2006; SCHOUSTRUP *et al.* 2006; VELICER *et al.* 2006) offer a powerful context for studying the genetics of evolutionary adaptation, because one can couple changes in phenotypic traits, including fitness and its components, with specific mutations. In these studies, it is of interest to know whether independent populations, when confronted with the same environmental challenges, will evolve along parallel or divergent paths. The convergence of multiple evolving lines on similar phenotypes provides a strong indication that the changes are adaptive as opposed to the product of random genetic drift (BULL *et al.* 1997; FERA *et al.* 1999; WICHMAN *et al.* 1999; COOPER *et al.* 2001, 2003; COLOSIMO *et al.* 2005; WOOD *et al.* 2005; PELOSI *et al.* 2006; WOODS *et al.* 2006).

Previous studies on evolutionary adaptation to stressful environments have focused on how known stress-responsive genes evolve (RIEHLE *et al.* 2001; DE VISSER *et al.* 2004). However, relatively few genes have been

identified that are known to be important for adaptation to freeze–thaw (FT) stress, especially in mesophilic organisms such as *Escherichia coli*. When populations of *E. coli* are subjected to repeated FT cycles, no survivors remain in the population after 40 cycles (SLEIGHT *et al.* 2006). To study how such populations may genetically adapt to these conditions over evolutionary time, 15 populations evolved under a freeze–thaw–growth (FTG) regime, where the growth phase allows for the selection of cells that can both survive and recover from the FT stress (SLEIGHT and LENSKI 2007). Here, we examine the genetic basis of evolutionary adaptation that occurred in these 15 FTG-evolved populations. The evolved lines achieved large increases in fitness relative to their progenitors when competed under the FTG regime, and these gains resulted from both improved survival after the FT cycle and faster recovery to initiate exponential growth after thawing (SLEIGHT and LENSKI 2007). This shorter lag phase is specific to recovery after freezing and thawing and not some more general improvement in recovery of growth following stationary phase *per se*. Thus, it is of interest to identify and characterize the genetic changes responsible for these adaptations to the FTG regime.

Various approaches have been used to find beneficial mutations substituted in bacterial evolution experiments (TREVES *et al.* 1998; PAPADOPOULOS *et al.* 1999; SCHNEIDER *et al.* 2000; COOPER *et al.* 2001, 2003; ZINSER

¹Corresponding author: Department of Bioengineering, University of Washington, Seattle, WA 98195. E-mail: sleight@u.washington.edu

et al. 2003; SCHNEIDER and LENSKI 2004; HERRING *et al.* 2006; PELOSI *et al.* 2006; VELICER *et al.* 2006). In this study, we screened the entire genomes of many of the FTG-evolved lines and their progenitors by using a fingerprinting approach with insertion sequence (IS) elements as probes. This approach led to the discovery of multiple IS-associated mutations at each of two loci, and these genes and mutations were further analyzed in this study at both the phenotypic and the molecular levels. In the paragraph below, we describe some of the salient features of IS elements relevant for our work.

IS elements are generally small (<2.5 kb) mobile genetic elements, found in bacteria, that carry information related only to their transposition and its regulation (MAHILLON and CHANDLER 1998). The number and locations of IS elements vary among bacterial genomes (DEONIER 1996; SCHNEIDER *et al.* 2002), and these elements are a significant source of new mutations (NAAS *et al.* 1994; HALL 1999; PAPADOPOULOS *et al.* 1999; SCHNEIDER *et al.* 2000; COOPER *et al.* 2001; DE VISSER *et al.* 2004; SCHNEIDER and LENSKI 2004). IS-mediated mutations can cause genomic rearrangements and also have diverse effects on gene expression (JORDAN *et al.* 1968; REYNOLDS *et al.* 1981; CHARLIER *et al.* 1982; CIAMPI *et al.* 1982; JAURIN and NORMARK 1983; BLASBAND *et al.* 1986; HALL 1999; BONGERS *et al.* 2003). Some authors have suggested that IS transposition may occur at higher rates in bacteria under various stressful conditions (REIF and SAEDLER 1975; NAAS *et al.* 1995; EICHENBAUM and LIVNEH 1998; HALL 1999; DE VISSER *et al.* 2004; OHTSUBO *et al.* 2005; TWISS *et al.* 2005), but IS-mediated mutations certainly occur in nonstressful environments as well (PAPADOPOULOS *et al.* 1999). In this study, we seek to determine whether IS mutations that were substituted in the evolving lines contributed to their adaptation to the FTG regime.

MATERIALS AND METHODS

Derivation of bacterial strains: The bacteria used in this study derive from a common ancestor via two successive evolution experiments, as summarized in Figure 1. In the first experiment, 12 populations independently evolved for 20,000 generations (3000 days) starting from two variants of the same ancestral strain of *E. coli* B (LENSKI *et al.* 1991; LENSKI 2004). One ancestral variant (REL606) cannot grow on arabinose, while the other (REL607) is a spontaneous Ara⁺ mutant. The Ara marker is selectively neutral under the conditions of that long-term experiment (LENSKI *et al.* 1991) as well as in the freeze-thaw-growth environment used in this study (SLEIGHT and LENSKI 2007). For the purposes of this article, we refer to both variants as the “ancestor,” unless we need to discriminate between them for methodological reasons, or as the “original ancestor” to minimize confusion with clones derived from the first evolution experiment that served as progenitors for the second evolution experiment. The long-term experiment involves daily transfers in Davis minimal medium supplemented with glucose at 25 µg/ml (DM25) with incubation at 37°. The 100-fold dilution and regrowth allow ~6.6 (= log₂ 100) generations per day. One clone was sampled from

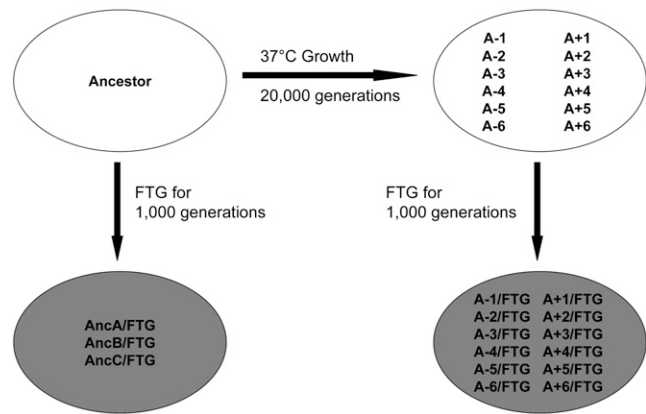


FIGURE 1.—Evolutionary histories of freeze-thaw-growth (FTG) populations. The ancestor of a long-term evolution experiment (LENSKI *et al.* 1991) was used to found 3 FTG-evolved populations. Twelve other FTG-evolved populations were founded by clones sampled from each of 12 populations that previously evolved for 20,000 generations at 37°. All 15 of the FTG lines evolved for 1000 generations under the FTG regime, with alternating days of a FT cycle and growth at 37°. The culture medium used for growth was the same as the one used in the long-term evolution experiment.

each of the 12 populations after 20,000 generations, and these 12 clones are designated as A-1–A-6 and A+1–A+6 for this study.

The second evolution experiment involves 15 populations that were propagated under the Ara⁺ FTG regime. Three populations were founded by the Ara⁺ variant of the original ancestor, and a single population was founded by each clone sampled from each of the 12 long-term populations. We used the long-term populations as progenitors for this FTG evolution experiment because, relative to the ancestor, we hypothesized they had more potential for evolutionary adaptation specific to the FT component of the cycle because they were already well adapted to benign growth conditions. Indeed, this hypothesis was well supported (SLEIGHT and LENSKI 2007). These 15 populations evolved for 150 2-day FTG cycles, which equals at least 1000 generations on the basis of the 100-fold dilution and growth in alternating days. Somewhat more generations occurred because growth also offset death during the freeze-thaw cycle in alternating days. To start the FTG evolution experiment, 1 ml of DM25 stationary-phase culture was transferred into a freezer tube and put in a –80° freezer for 22.5 hr. The tube then thawed at room temperature (~22°) for 1.5 hr, after which time the culture was diluted 100-fold into fresh DM25 and incubated at 37° without shaking for 24 hr. Thus, the evolving populations experienced cycles of a day of freezing and thawing that alternated with a day of growth in the same medium and at the same temperature as during the long-term evolution experiment. Populations and clones were sampled and stored every 100 generations (30 days) in freezer vials with glycerol for future studies. Note that glycerol was added as a cryoprotectant for long-term storage of samples, but no cryoprotectant was present during the actual FTG-evolution experiment itself. The three populations derived from the original ancestor are designated as AncA/FTG, AncB/FTG, and AncC/FTG, while the other 12 are designated as A-1/FTG–A-6/FTG and A+1/FTG–A+6/FTG (Figure 1).

During the first evolution experiment, unique mutations were substituted in each of the 12 populations after 20,000 generations, including different alleles in *nadR* (WOODS *et al.*

2006). To check for the possibility of inadvertent cross-contamination during the second evolution experiment, the *nadR* gene was resequenced in all 15 of the FTG lines. In all cases, the *nadR* alleles precisely matched that of their intended progenitors, thereby excluding any cross-contamination.

DNA extractions, PCR, and sequencing: DNA was extracted from cultures grown overnight in LB medium using the QIAGEN (Valencia, CA) genomic-tip 100/G kit and quantified using a spectrophotometer. Polymerase chain reaction (PCR) was performed using the Promega (Madison, WI) High Fidelity Taq Polymerase kit in a PTC-200 thermocycler (MJ Research, Watertown, MA). PCR products were purified using a GFX PCR DNA and gel band purification kit (Amersham Biosciences, Arlington Heights, IL). Purified PCR products were sequenced by the dideoxy chain termination method (SANGER *et al.* 1977). DNA sequences were aligned in the SeqMan program (DNASTAR, Madison, WI). All mutations were verified by repeating this entire process at least twice.

Southern hybridizations with IS probes: Extracted genomic DNA from each clone was digested with *EcoRV* (for IS1, IS2, IS3, IS4, IS30, and IS186) or *HincII* (for IS150), separated on a 0.8% agarose gel with a 1-kb ladder (New England Biolabs, Beverly, MA), and transferred to nylon membranes (SOUTHERN 1975). Hybridizations were performed at high stringency (68°), using as probes internal fragments of each IS, which were PCR amplified using primers shown in supplemental Table 1, purified, and labeled using the DIG DNA labeling and detection kit (Roche, Indianapolis).

Characterization of sequences adjacent to IS elements by inverse PCR: Genomic DNA from each clone was digested with *EcoRV* or *HincII* and separated on agarose gels. Gel fragments containing IS elements were cut and purified using the GFX PCR DNA and the gel band purification kit (Amersham Biosciences). The fragments were self-ligated using T4 DNA Ligase (New England Biolabs) at 10 µg/ml, and the ligated mixtures were used as templates in PCR reactions, using primers directed outward from the appropriate IS element (supplemental Table 2). PCR products were purified and sequenced, and the sequences adjacent to the IS element were compared to the genome sequence for *E. coli* K-12 (RILEY *et al.* 2006; GenBank accession no. NC_000913). Once these adjacent sequences were identified, primers were designed to PCR amplify the IS-insertion allele on the chromosome. The PCR products were sequenced with the same primers (supplemental Table 2) to determine the exact position, orientation, and target-site duplication caused by the IS insertion.

Isogenic strain construction: Isogenic constructions and reconstructions were created using the “gene-gorging” replacement technique (HERRING *et al.* 2003). In the case of the A-2/FTG evolved clone, which has an 11-bp deletion in the *cls* gene, we performed two allelic replacements. First, the ancestral *cls* allele was moved into this evolved clone. Next, the evolved clone with the introduced ancestral *cls* allele was reconstructed to the evolved *cls* deletion allele to verify that phenotypic differences were caused by the mutation and not a side effect of the gene-gorging process. Second, the evolved *cls* deletion allele was moved into the A-2 progenitor and then reconstructed back to the ancestral *cls* allele. We used the A-2/FTG line, rather than other evolved lines that had IS insertions in the *cls* gene, because this 11-bp deletion is easier to manipulate. In the case of the AncB/FTG-evolved clone, which acquired an IS150 insertion in the *uspA/B* intergenic region, we independently made two isogenic constructs from which this IS150 insertion was removed, thereby restoring the ancestral allele of *uspA/B*. In this case, we did not move the *uspA/B*:IS150 allele back into this construct, or into the ancestor, because recombination events that occur during the strain construction process with other IS150 copies already present in the chromo-

some make such constructions problematic. The two independently constructed isogenic strains from which the IS150 insertion was removed did not differ significantly from one another in any respect, supporting their isogenicity, and the data obtained for them are combined in the competition and real-time PCR experiments reported in this article.

For all constructs, we used one primer with an *I-SceI* restriction site on its 5' end. Fragments that included ~500 bp on each side of the mutation site or its ancestral equivalent were PCR amplified and purified. Primers used to make the *cls* and *uspA/B* constructs are available in supplemental Table 3. The resulting ~1-kb fragment was cloned into pCRII-Topo and transformed into *E. coli*, using the Topo TA cloning kit (Invitrogen, San Diego). Transformants were selected and grown in LB supplemented with ampicillin, and the plasmids were purified using the Promega Wizard Plus SV Miniprep DNA purification system. All cloned fragments were checked by DNA sequencing, and no additional mutations were detected.

Recombination of the different alleles into the chromosome was performed as described by HERRING *et al.* (2003). Putative constructs were then screened for the desired genotype, using PCR with primers specific to the corresponding gene.

Quantifying FTG fitness and its components: We performed competition experiments to measure the relative fitness levels of various ancestral, evolved, and constructed genotypes. The neutrally marked variants of the ancestral strain allowed competitors to be distinguished on the basis of colony color on tetrazolium–arabinose (TA) indicator agar (LENSKI *et al.* 1991; SLEIGHT and LENSKI 2007). For each replicate competition assay, each competitor's realized (net) growth rate, r , was measured over the 2-day FTG cycle, as

$$r = \ln((N_2 \times 100)/N_0),$$

where N_2 is that competitor's final cell density, N_0 is its initial cell density, and the factor of 100 takes into account the 100-fold dilution between each FTG cycle. Thus, the overall FTG fitness of one competitor relative to another is simply the ratio of their respective realized growth rates over the complete cycle.

We also calculated each competitor's FT survival, s , and subsequent growth rate, g , over the 2 separate days of the FTG cycle as

$$s = N_1/N_0$$

$$g = \ln((N_2 \times 100)/N_1),$$

where N_1 is the viable cell density measured after the first day of the cycle prior to the 100-fold dilution. Note that survival is a proportion, whereas growth is a rate. In any case, the relative survival and growth of two competitors are expressed as the ratio of the relevant parameters, so that both become dimensionless quantities, as is the overall FTG fitness. Note also that all of these quantities are calculated separately for each replicate assay, thus preserving their statistical independence. The quantities were averaged across replicates and analyzed statistically as described below.

Statistical methods: We performed paired *t*-tests to compare the properties of two clones, with pairing based on temporal and spatial proximity in the structure of the experiment. In those cases where we had *a priori* expectations about the direction of change, significance was computed using one-tailed *t*-tests; otherwise two-tailed tests were used. We expected the FTG-evolved lines to have improved performance relative to their progenitors in the FTG regime, including both FT survival and subsequent growth. We also expected that evolved

alleles would confer an advantage under the FTG conditions and when present in the evolved genetic background. However, we had no expectations for other phenotypic aspects of isogenic clones differing only by a specific allele. Two-way ANOVAs were performed to compare phenotypic measures between clones with the four combinations of ancestral and evolved backgrounds and alleles.

Measuring membrane fluidity: Fluorescence polarization (anisotropy) measures fluidity in the cytoplasmic membrane using various probes, each one specific to a particular region of the membrane (HARRIS *et al.* 2002; VANOUNOU *et al.* 2002). Fluorescence anisotropy was measured with a Spectramax M5 fluorometer (Molecular Devices, Menlo Park, CA) using two probes, 6-dodecanoyl-2-dimethylaminoaphthalene (laurdan) and 1,3-diphenyl-1,3,5-hexatriene (DPH). Laurdan is an amphipathic molecule that localizes near the lipid polar head groups in the cytoplasmic membrane and is therefore sensitive to changes at the water–lipid interface (HARRIS *et al.* 2002; VANOUNOU *et al.* 2002). DPH is useful for detecting changes in saturation of fatty acyl chains in the cytoplasmic membrane (ARICHA *et al.* 2004; BENEY *et al.* 2004). Either laurdan (5×10^{-5} M added from a stock solution in methanol) or DPH (5×10^{-5} M added from a stock solution in tetrahydrofuran) was incubated for 1 hr at room temperature in the dark with 0.2 ml of cultures sampled either at stationary phase or after a FT cycle. Cultures without any probe were used as a scattering control and were incubated under the same conditions, for each individually measured sample.

The ratio of probe to culture concentration was chosen by using the minimum concentration giving an appropriate signal-to-noise ratio (VANOUNOU *et al.* 2002). Laurdan anisotropy was measured at the 355-nm excitation wavelength and 440-nm emission wavelength. DPH anisotropy was measured at the 360-nm excitation wavelength and 430-nm emission wavelength. Anisotropy (r) is calculated as

$$r = (I_V - GI_H)/(I_V + 2GI_H),$$

where I_V and I_H are the fluorescence intensities determined at vertical and horizontal orientations of the emission polarizer when the excitation polarizer is set in the vertical position (HARRIS *et al.* 2002). G is a correction factor for dissymmetry associated with the horizontal and vertical positions of the polarizers. Lower anisotropy values indicate higher probe rotation and thus imply a more fluid membrane compared to higher anisotropy values.

RNA extractions and real-time PCR: RNA was extracted from cultures at stationary phase (24 hr after dilution into fresh media), after a FT cycle (frozen at -80° for 22.5 hr and then thawed for 1.5 hr at room temperature), and under transitional growth conditions (2 hr after the thawed culture was diluted 1:10 into DM25 and incubated at 37°), using the RNeasy mini kit (QIAGEN). For that third treatment, 2 hr was chosen because the ancestor is still deep within its long FT-associated lag phase, whereas the evolved clone is approaching the time when it starts growth (SLEIGHT and LENSKI 2007); hence, that time point may reveal physiologically important differences in gene expression between the evolved clone and the ancestor. A 1:10 dilution was used, instead of the 1:100 dilution used in the evolution experiment, to extract enough RNA for the real-time (RT)–PCR procedure; control experiments confirmed that the difference between the ancestor and the evolved clone in the duration of their lags after a FT cycle is comparable for 1:10 and 1:100 dilutions. The same culture volume was used for each clone to preserve the relevant cell density, while an endogenous control served to measure the total RNA present (see below). After extraction, RNA was treated with RNase-free DNase (Ambion, Austin, TX), and

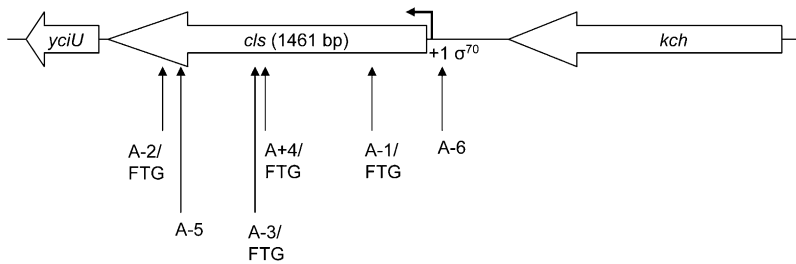
PCR experiments were run using the extracted RNA as a template to ensure the absence of DNA in the RNA samples. RT–PCR was performed using the TaqMan One-Step RT–PCR kit (Applied Biosystems, Foster City, CA) with primers and MCB probes specific to the *uspA*, *uspB*, and 16S rRNA genes in the ABI Prism 7900HT sequence detection system. Negative controls without any RNA were also used in RT–PCR experiments, and they produced no significant background noise. An RNA standard was obtained by mixing RNA from different samples, and a \log_{10} dilution series through 10^{-5} was measured with the primers and probe for each gene. Regression was then performed on C_T (threshold cycle) values against the dilution factor to determine the amount of RNA in unknown samples. The mRNA levels for *uspA* and *uspB* levels were individually divided by the 16S rRNA levels for each clone and sample time point to ensure that any differences were not an artifact of the total amount of RNA extracted.

Ethanol sensitivity experiments: Samples of an evolved clone in stationary phase or after a FT cycle were mixed with the reciprocally marked ancestor from the same condition, as in a competition experiment. The mixed culture was then incubated in 10% ethanol at 37° for 1 hr. Cell densities were measured before and after ethanol exposure and used to quantify relative sensitivity, using the same equation used to quantify relative FT survival.

RESULTS

Discovery of several IS-associated mutations in FTG-evolved lines: To characterize genetic changes and genomic rearrangements associated with IS elements in FTG-evolved lines relative to their progenitors, a restriction fragment length polymorphism (RFLP) analysis was performed using internal fragments from each of the seven IS elements in *E. coli* B as probes. One clone sampled from 10 of the 15 evolved FTG populations was compared against its progenitor for each of the seven IS elements (supplemental Table 4). An IS-associated change is defined as either a gain or a loss of a band; however, one IS-mediated mutation can produce more than one band change, and therefore this method may sometimes overestimate the number of underlying mutational events (PAPADOPOULOS *et al.* 1999; SCHNEIDER *et al.* 2000). Of the seven IS elements, three showed no changes (IS2, IS4, and IS30) in any of the 10 evolved lineages. By contrast, there were 30 total changes in the other four IS elements (IS1, IS3, IS150, and IS186), with IS150 alone contributing more than half of these changes. This high level of activity is not specific to FTG conditions, because IS150 also shows high activity under benign growth conditions (PAPADOPOULOS *et al.* 1999; SCHNEIDER *et al.* 2000; COOPER *et al.* 2001).

Localization of IS-associated mutations in FTG-evolved lines: Given the numerous IS-associated mutations that we found, we focused our attention on characterizing those changes that arose independently in multiple FTG-evolved lines. Supplemental Figure 1 shows the Southern hybridizations using the IS150 sequence to probe the genomes of the FTG-evolved lines and their progenitors. Bands present in more than



each population. The bent arrow indicates the putative transcription start site of *cls*, and the sigma factor (σ^{70}) responsible for its transcription is also shown (IVANISEVIC *et al.* 1995). The *yciU* gene (330 bp) encodes a hypothetical protein and is predicted to be transcribed in the same direction as *cls*. In this case, the *cls* mutations may have polar effects on *yciU* transcription. The *kch* gene (1254 bp) encodes a potassium voltage-gated ion channel.

one FTG-evolved line, but not in their progenitors, are circled and the chromosomal location is indicated. Two of the 10 FTG-evolved clones that were tested have an insertion in the *cls* gene, and 4 evolved clones have an insertion in the *uspA/B* intergenic region.

Systematic screening of *cls* mutations in FTG-evolved lines: After the *cls* and *uspA/B* insertion mutations were discovered, we screened 10 clones from each of the 15 FTG-evolved populations for the presence of insertion mutations in these loci, using PCR with primers designed to detect mutations in regulatory as well as coding regions. For the *cls* gene, 5 FTG-evolved lines were found to have IS insertions in at least one clone, including the 2 lines in which *IS150* insertions were originally found (A+4/FTG and A-3/FTG). In a third line (A-1/FTG), an *IS150* insertion was found in a single clone that was not tested in the previous Southern hybridizations. In 2 other lines (A-5/FTG and A-6/FTG), all clones tested had insertions of a different element, *IS186*, either in or immediately upstream of *cls*. Surprisingly, however, the progenitors of these 2 lines (A-5 and A-6), which had evolved for 20,000 generations at constant 37°, already harbored the *cls::IS186* insertions. Thus, while these last two mutations might have contributed to adaptation to the previous environment, they cannot be responsible for the fitness gains specific to the FTG regime. In all of the other FTG-evolved lines that had no insertion mutations in *cls*, we sequenced that gene and its adjacent regulatory region. One additional substitution was found, in which the A-2/FTG-evolved line had an 11-bp deletion that generates a premature stop codon 105 bp upstream of the original one. The physical locations of all these *cls* mutations and the number of mutated clones in each population are listed in supplemental Table 5, while Figure 2 provides a schematic. We presume that all of the *cls* mutations that evolved during the FTG experiment, including the deletion in line A-2/FTG, disrupt the function of the encoded enzyme, cardiolipin (CL) synthase. This enzyme is widely distributed across bacterial species, and it converts two phosphatidylglycerol molecules into CL and glycerol in the membrane (HIRSCHBERG and KENNEDY 1972) during stationary phase (SHIBUYA and HIRAOKA 1992).

FIGURE 2.—Schematic of mutations in *cls*. Block arrows indicate the direction of transcription for each gene and are drawn to scale. Upward pointing arrows indicate the location of *IS150* (A+4/FTG, A-1/FTG, A-3/FTG) and *IS186* (A-5, A-6) insertions and an 11-bp deletion (A-2/FTG) in FTG-evolved clones or progenitors already harboring insertions. See supplemental Table 5 for information on the location of each mutation and the number of mutated clones in

Systematic screening of *uspA/B* mutations in FTG-evolved lines: By screening the same 10 clones from each of the 15 FTG-evolved lines, we found mutations in *uspA/B* and its associated regulatory region in one or more clones in 8 different populations. Strikingly, all of the mutations were *IS150* insertions in the same exact position and orientation in the *uspA/B* intergenic region (Figure 3, supplemental Table 5). Cross-contamination can be ruled out as a possible explanation because these clones have different IS banding patterns in RFLP experiments, different *cls* mutations (as described above), and unique *nadR* alleles derived from their progenitors (see MATERIALS AND METHODS). Figure 3 shows that these identical *IS150* insertions are located 34 bp upstream of the *uspB* start codon and 95 bp downstream of the putative *uspB* σ^S -promoter. The *uspA* and *uspB* genes encode universal stress proteins (Usp) A and B, respectively. UspA is an autophosphorylating serine and threonine phosphoprotein that is induced under a wide variety of stress conditions; it is thought to play a role in protecting cells from DNA damage, although its exact function is unknown (KVINT *et al.* 2003). Even less is known about UspB, although it is differentially transcribed from UspA and might not be a truly universal stress protein (FAREWELL *et al.* 1998; KVINT *et al.* 2003). In the 7 other FTG lines without *uspA/uspB::IS150* mutations, we sequenced *uspA*, *uspB*, and the *uspA/B* intergenic region for individual clones, but found no other mutations.

Phenotypic effects of evolved *cls* mutation: We performed two types of experiments to investigate the physiological effects of the *cls* deletion mutation in the evolved and progenitor backgrounds: fitness assays and membrane fluidity measurements.

Fitness assays: We measured the relative fitness levels of all four isogenic strains, including the ancestral and evolved *cls* alleles in the progenitor and FTG-evolved genetic backgrounds, under four conditions (Figure 4): over the entire 2-day FTG regime, FT survival only, growth performance after the FT treatment only, and growth performance after stationary phase (without a FT cycle). Over the entire FTG cycle, the evolved clone with the *cls*⁻ mutation has a significantly higher fitness

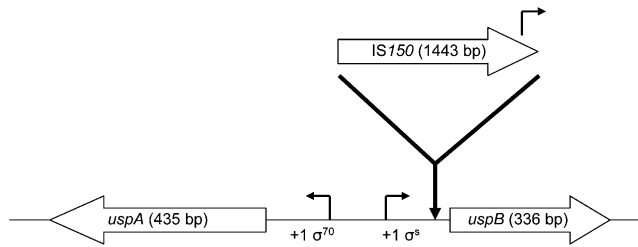


FIGURE 3.—Schematic of IS150 insertions in the *uspA/B* intergenic region. Block arrows indicate the direction of transcription for each gene and are to scale except for the IS150 element. Eight of the 15 FTG populations had at least one tested clone with an IS150 insertion in the exact same position and orientation, 34 bp upstream of the *uspB* start codon. This insertion generated a 3-bp duplication at the target site and is 95 bp downstream of the putative *uspB* promoter (σ^5). The IS150 element has at least one possible promoter-like sequence directed outward (SCHWARTZ *et al.* 1988) toward *uspB*. See supplemental Table 5 for information on the location of this mutation and the number of mutated clones in each population.

than its progenitor with the ancestral *cls*⁺ allele (Figure 4A; paired one-tailed *t*-test, $P < 0.0001$). This higher overall fitness reflects both improved FT survival and subsequent growth after the FT treatment (Figure 4, B and C; paired one-tailed *t*-tests, $P = 0.0001$ and 0.0006 , respectively). This overall improvement is specific to FTG conditions, because the evolved clone has a small, but significant, decrease in its performance without the FT treatment (Figure 4D; paired two-tailed *t*-test, $P = 0.0038$). Note the scale differences between sections in Figure 4; therefore, the error bars on the fitness values that are not significantly different from 1.0 in Figure 4D are, in fact, very tight. These comparisons demonstrate that the evolved A-2/FTG line improved its FTG fitness relative to its progenitor and that its adaptation is specific to the FTG regime.

Restoring the ancestral *cls*⁺ mutation to this evolved strain reduces overall FTG fitness by ~24% (Figure 4A; paired two-tailed *t*-test, $P = 0.0002$). The evolved allele significantly improves both FT survival and subsequent growth (Figure 4, B and C; paired two-tailed *t*-tests, $P = 0.0054$ and 0.0024 , respectively). Moreover, the improvement associated with the evolved *cls* allele is specific to the FTG regime, as there is no significant difference between the ancestral *cls*⁺ and evolved *cls*⁻ alleles in the same evolved A-2/FTG genetic background during competition after stationary phase without a FT cycle (Figure 4D; paired two-tailed *t*-test, $P = 0.5077$). These comparisons demonstrate that the *cls*⁻ allele contributes significantly to the FTG-specific adaptation.

When moved into the A-2 progenitor background, however, the same evolved *cls*⁻ allele shows a much smaller (~5%) and marginally nonsignificant advantage in overall FTG fitness (Figure 4A; paired two-tailed *t*-test, $P = 0.0957$). Also, neither FT survival nor sub-

sequent growth after FT treatment shows any significant effect of the *cls* allele in the progenitor background (Figure 4, B and C; paired two-tailed *t*-tests, $P = 0.4686$ and 0.2736 , respectively). The ancestral *cls*⁺ allele has a small, but again nonsignificant, advantage during growth after stationary phase without the FT cycle (Figure 4D; paired two-tailed *t*-test, $P = 0.1250$). Evidently, the fitness effects of the evolved *cls*⁻ allele are contingent on interactions with one or more other mutations in the evolved A-2/FTG line. This conclusion is further supported by a two-way ANOVA using the overall FTG fitness data, which indicates a highly significant interaction between the genetic background and the *cls* allele ($P = 0.0001$). Growth-curve experiments performed both after stationary phase and after a FT cycle are consistent with fitness measurements (SLEIGHT 2007).

Membrane fluidity: Previous research has shown that *cls* mutants have altered membrane phase transitions during or after a temperature downshift (PLUSCHKE and OVERATH 1981). To test whether the evolved *cls*⁻ allele also changes membrane fluidity, we measured fluorescence anisotropy of the same four strain constructs after either FT treatment or stationary phase at 37° (see MATERIALS AND METHODS for further details). Laurdan is a fluorescent probe that localizes to the cytoplasmic membrane and that is sensitive to changes in the water-lipid interface where the phospholipid head groups reside (HARRIS *et al.* 2002; VANOUNOU *et al.* 2002). The results of the experiments are summarized in Figure 5.

Figure 5A shows that the evolved *cls*⁻ allele significantly increases membrane fluidity (reduces laurdan anisotropy) relative to the ancestral *cls*⁺ allele following FT treatment and does so in both the progenitor and the FTG-evolved backgrounds. One or more other evolved alleles must also contribute to greater membrane fluidity, because the evolved construct has greater fluidity than the progenitor even when both strains have the same ancestral *cls*⁺ allele. A two-way ANOVA indicates the effects of both genetic background and the *cls* allele are highly significant, while there is no significant interaction with respect to this phenotype (Table 1). The evolved *cls*⁻ allele therefore increases membrane fluidity after freezing and thawing regardless of genetic background. However, recall from the fitness experiments that the evolved *cls*⁻ allele was much more beneficial under the FTG regime in the evolved background. Taken together, these findings indicate that the benefit of increased membrane fluidity after the FT cycle must depend, at least in part, on other mutations in the A-2/FTG-evolved line.

We see no significant differences in membrane fluidity when laurdan anisotropy is measured for the same four strains after stationary phase, without the FT treatment (Figure 5B, two-way ANOVA for genetic background and allele; main effects and interaction

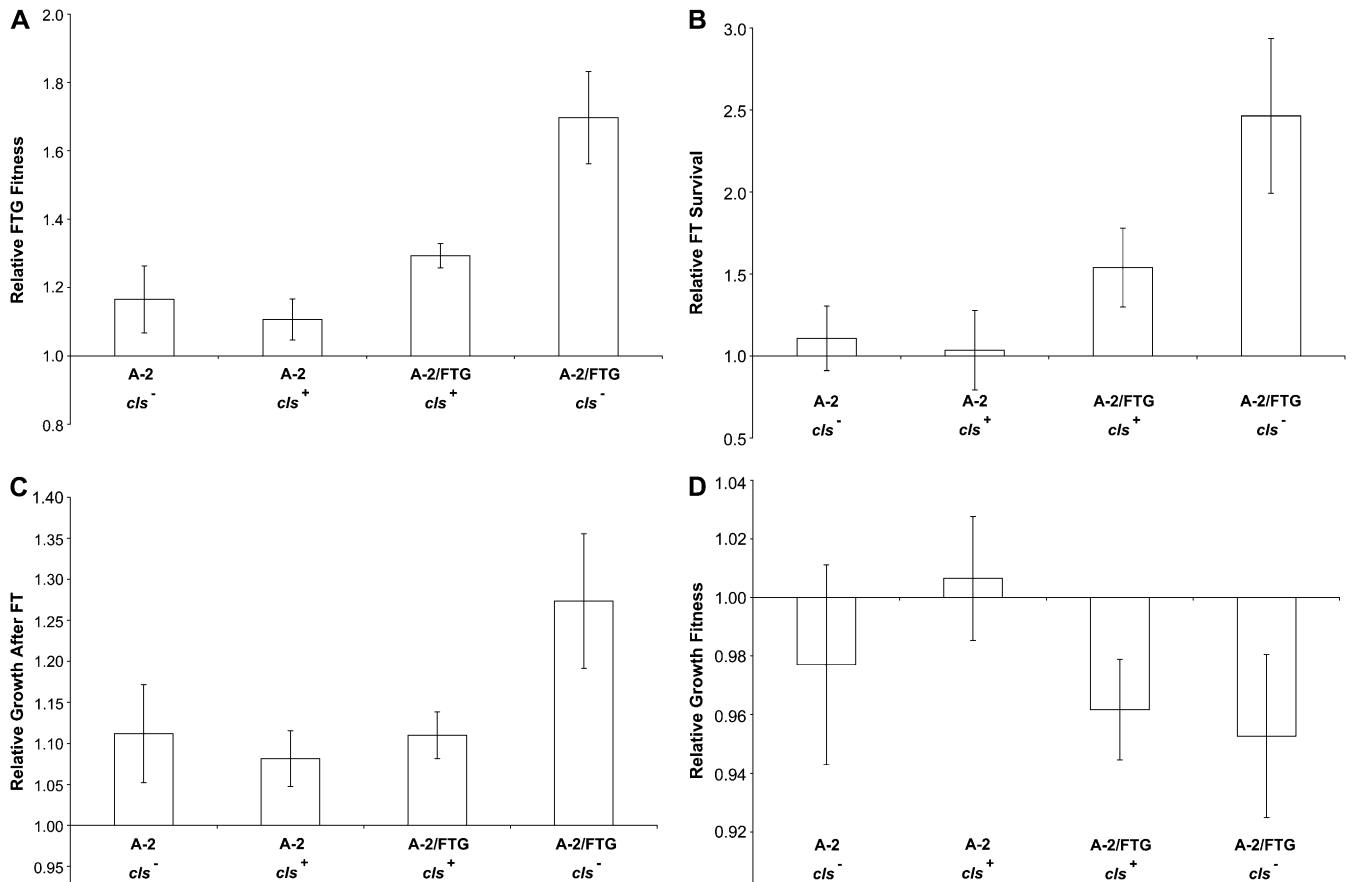


FIGURE 4.—Relative fitness components of the following clones: A-2 *cls*⁻ construct, A-2 *cls*⁺ progenitor, A-2/FTG *cls*⁺ construct, and A-2/FTG *cls*⁻ evolved clone. All four types competed against an Ara⁺ mutant of the A-2 progenitor. Fitness components are as follows: (A) overall FTG fitness, (B) FT survival, (C) growth after FT, and (D) growth after stationary phase. Error bars are 95% confidence intervals based on eight replicate assays.

$P > 0.35$). Therefore, the effect of the evolved *cls*⁻ allele on membrane fluidity is specific to freezing and thawing. Note also that the anisotropy value of the A-2/FTG-evolved strain, with its evolved *cls*⁻ allele, is almost the same when measured after the FT treatment as it is following stationary phase at 37°. This similarity indicates that the FTG-evolved line can maintain its membrane fluidity at the water–lipid interface after a FT cycle, whereas the progenitor’s membrane (especially with the ancestral *cls*⁺ allele) becomes much more rigid.

We also used the same approach to measure changes in membrane fluidity in two of the FTG-evolved lines with IS150 insertions in the *cls* gene (A+4/FTG and A-3/FTG) relative to their respective progenitors. Both of these evolved lines also have significantly increased membrane fluidity relative to their progenitors after a FT cycle, but not during stationary phase (SLEIGHT 2007), paralleling the case of the A-2/FTG-evolved clone with the *cls* deletion relative to its progenitor (Figure 5). By contrast, the two FTG-evolved lines whose progenitors (A-5 and A-6) already had IS186 insertions in or near the *cls* gene (Figure 2) evolved no further changes in their membrane fluidity

following the FT treatment (SLEIGHT 2007). Taken together, these results indicate that the *cls* mutations are a major, but not the sole, determinant of the evolved changes in membrane fluidity measured after the FT treatment.

To this point, our experiments on membrane fluidity have used laurdan as a probe that is sensitive to changes at the water–lipid interface. We also performed fluorescence polarization measurements using the probe DPH, which is used to detect differences in fatty acyl chains in the membrane. However, we found no differences between multiple FTG-evolved lines and their progenitors, either during stationary phase or after the FT treatment, when using DPH as a probe (SLEIGHT 2007).

Phenotypic effects of evolved *uspA/B* mutation: We constructed isogenic strains, in an evolved background only, by replacing the *uspA/uspB::IS150* allele in clones from the AncB/FTG-evolved line with the *uspA/B* ancestral allele. The derived strains were analyzed in two ways: fitness assays and transcription quantitation.

Fitness assays: Figure 6 shows the relative fitness values measured for the ancestor (without the IS insertion), the AncB/FTG-evolved line with its evolved *uspA/B::IS150*

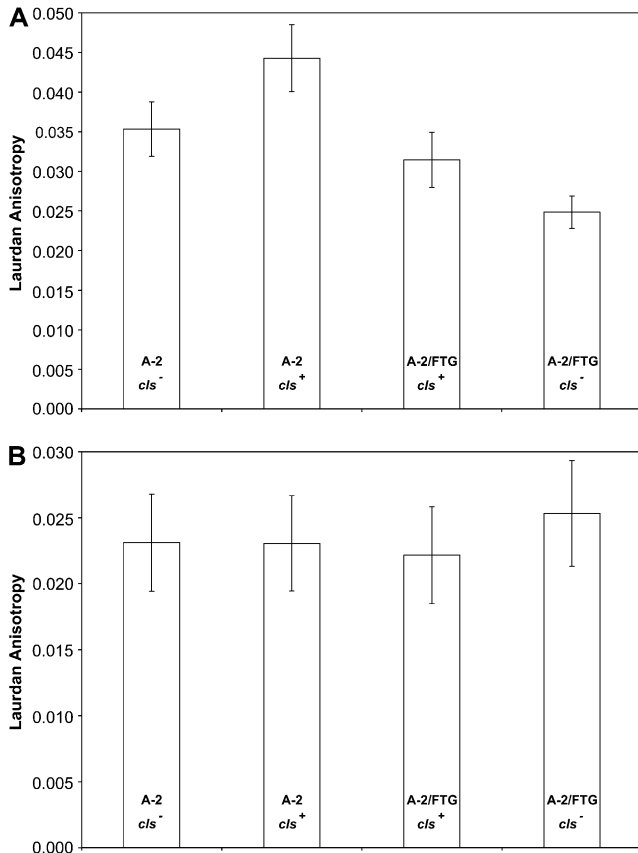


FIGURE 5.—Laurdan anisotropy differences following (A) FT treatment and (B) stationary phase. Each clone was incubated with the fluorescent probe laurdan, and fluorescence anisotropy was measured individually in a fluorometer with 18-fold replication. Lower anisotropy values are indicative of a more fluid membrane in the context of the water–lipid interface. See MATERIALS AND METHODS for details.

allele, and the same evolved strain except with that *IS150* insertion replaced by the ancestral allele. As expected, the evolved clone has a large fitness advantage relative to its ancestor under the full 2-day FTG regime (Figure 6A; paired one-tailed *t*-test, $P < 0.0001$). Both FT survival and subsequent growth performance contribute significantly to the overall improvement (Figure 6, B and C; paired one-tailed *t*-tests, both $P < 0.0001$). Even without the FT cycle, this evolved line's fitness increased significantly (Figure 6D; paired one-tailed *t*-test, $P = 0.0003$), although much less so than under the FTG regime; the advantage after FT treatment was ~60% (Figure 6C) as compared to <5% following stationary phase at 37° (Figure 6D). Again, note the difference in scales between Figure 6C and 6D; the confidence intervals on the values in Figure 6D are very tight. The fact that this AncB/FTG-evolved line shows some nonspecific adaptation to the growth conditions, whereas the A-2/FTG line examined previously did not, is probably because AncB/FTG derives from the original ancestor, whereas A-2/FTG derives from a progenitor that had already evolved under the same growth conditions for 20,000 generations.

TABLE 1

ANOVA testing for effects of the *cls* allele, genetic background, and their interaction on laurdan anisotropy measured after freeze–thaw treatment

Source of variation	DF	SS	MS	F	<i>P</i>
Allele	1	0.00109	0.00109	23.457	<0.0001
Background	1	0.00245	0.00245	52.779	<0.0001
Allele × background	1	0.00002	0.00002	0.528	0.4700
Error	68	0.00316	0.00005		
Total	71	0.00672			

Eliminating the *IS150* insertion from the *uspA/B* intergenic region in the evolved clone (AncB/FTG –*IS150*) causes a small, but significant, reduction in FTG fitness (Figure 6A; paired two-tailed *t*-test, $P = 0.0022$). Both FT survival and growth performance after the FT cycle benefit from the presence of this insertion (Figure 6, B and C; paired two-tailed *t*-tests, $P = 0.0358$ and 0.0023 , respectively). The beneficial effect of the evolved *uspA/uspB::IS150* allele is specific to FTG conditions, as there is no advantage to the evolved clone of having the *IS150* insertion in growth after stationary phase without an intervening FT treatment; in fact, there is a marginally nonsignificant advantage when the evolved *uspA/uspB::IS150* allele is replaced by the insertion-free ancestral allele without the FT treatment (Figure 6D; paired two-tailed *t*-test, $P = 0.0685$). Again, growth-curve experiments performed both after stationary phase and after a FT cycle are consistent with fitness measurements (SLEIGHT 2007).

Transcription quantitation: We measured the transcription levels of both *uspA* and *uspB* by performing RT-PCR in stationary phase, after a FT cycle, and under growth-permissive conditions 2 hr after thawed cultures were diluted into fresh media (Figure 7). Under all three conditions, transcription of *uspB* is reduced by more than an order of magnitude in the evolved *uspA/B::IS150* allele relative to both the evolved strain with the ancestral *uspA/B* allele restored and the ancestor itself. By contrast, the evolved allele has only a small effect on *uspA* transcription under the same test conditions (SLEIGHT 2007). This difference is consistent with the physical location of the *IS150* insertion between the putative σ^S -promoter and start codon for *uspB*, whereas the upstream regulatory region for *uspA* is not interrupted by the insertion (Figure 3).

Although UspB is called a universal stress protein, it is evidently beneficial to reduce or even eliminate its expression for freeze–thaw survival and recovery. In fact, UspB is a predicted membrane protein, and *uspB* mutants are hypersensitive to ethanol during stationary phase (FAREWELL *et al.* 1998). Ethanol fluidizes membranes, and the physiological response to ethanol is an increase of membrane rigidity (DOMBEK and INGRAM 1984). We hypothesized, therefore, that the disruption

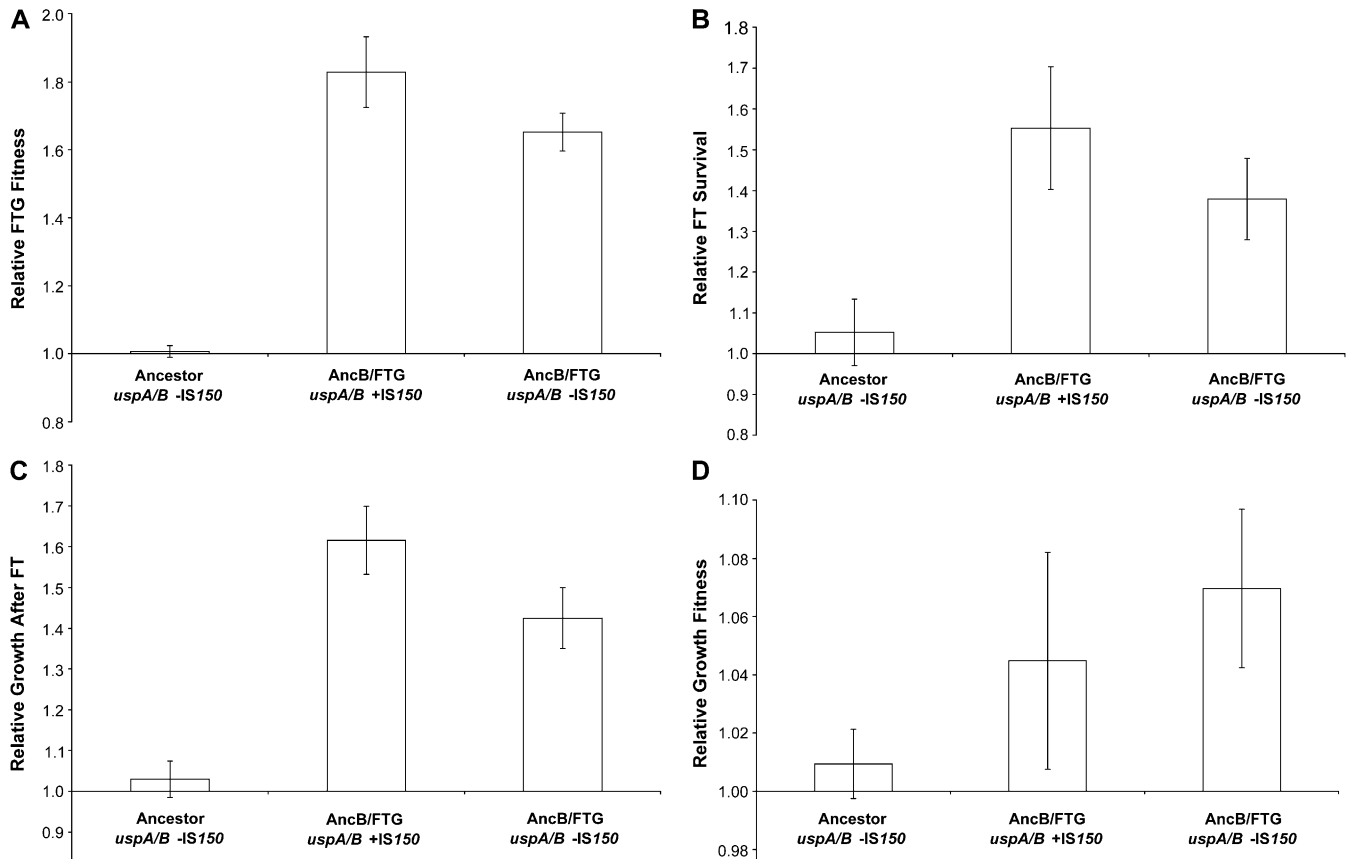


FIGURE 6.—Relative fitness components of the following clones: ancestor (*uspA/B* -IS150), evolved clone AncB/FTG *uspA/B* +IS150, and constructed clone AncB/FTG *uspA/B* -IS150. All three genotypes competed against the ancestor with the opposite arabinose marker. Each relative fitness component is as follows: (A) overall FTG fitness, (B) FT survival, (C) growth after FT, and (D) growth after stationary phase. Error bars are 95% confidence intervals of 12 replicate assays.

of *uspB* transcription increases membrane fluidity, which would be beneficial in the FTG regime, but should reduce survival during ethanol exposure. To test this hypothesis, we examined the predicted effects on membrane fluidity and ethanol sensitivity by comparing the isogenic strains with and without the IS150 insertion that disrupts *uspB* transcription. Possible differences in membrane fluidity were measured by performing fluorescence anisotropy after a FT cycle, as well as during stationary phase, using both laurdan and DPH as probes. However, we saw no significant differences in any of these cases (SLEIGHT 2007). The strains were also tested for differences in ethanol sensitivity during stationary phase or after a FT cycle, but we saw no significant differences between these strains under either treatment (SLEIGHT 2007). In summary, the IS150 insertion greatly reduces *uspB* transcription, which is beneficial under the FTG regime, but the physiological basis for that benefit remains unknown.

DISCUSSION

We screened the entire genomes of clones from many of the FTG-evolved lines and their progenitors by using

an RFLP method with native IS elements as probes (NAAS *et al.* 1994; PAPADOPOULOS *et al.* 1999; SCHNEIDER *et al.* 2000; COOPER *et al.* 2001; DE VISSER *et al.* 2004; SCHNEIDER and LENSKI 2004). This approach led to the discovery of new IS insertions and other mutations in multiple FTG-evolved lines at each of two loci, *cls* and *uspA/B* (Figures 2 and 3). Competitions between isogenic strains that differ only at these loci revealed that evolved alleles in both genes confer benefits that are specific to the FTG regime.

Physiological significance of the evolved mutations

in *cls*: The *cls* gene encodes the CL synthase enzyme, which catalyzes condensation of two phosphatidylglycerol (PG) molecules to form CL and glycerol (HIRSCHBERG and KENNEDY 1972). CL is one of the three main phospholipids in *E. coli*, the other two being phosphatidylethanolamine (PE) and PG (AMES 1968; CRONAN 1968; CRONAN and VAGELOS 1972). The relative amounts of these phospholipids depend on the physiological condition of cells; PG is most abundant in exponentially growing cells, while CL is dominant in stationary-phase cells and also under other conditions when cellular energy levels are lowered (AMES 1968; CRONAN 1968; CRONAN and VAGELOS 1972; HEBER and TRÖPP 1991;

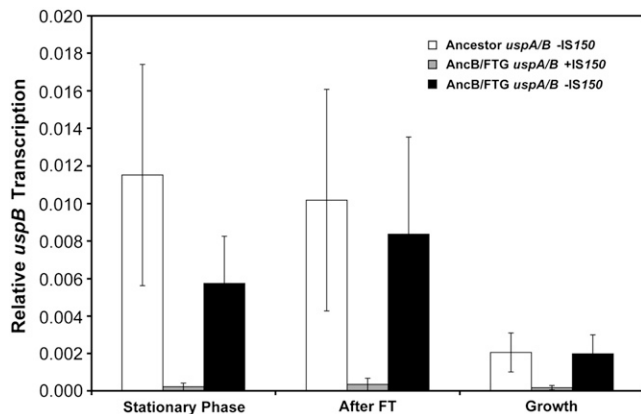


FIGURE 7.—Relative *uspB* transcription differences using real-time PCR. *uspB* transcription was measured relative to 16S rRNA transcription as an endogenous control at stationary phase, after a FT cycle, and under growth conditions 2 hr after thawed cultures were diluted into fresh media. Clones are as follows: ancestor *uspA/B* -IS150 (open bar), evolved clone AncB/FTG *uspA/B* +IS150 (shaded bar), and constructed clone AncB/FTG *uspA/B* -IS150 from which the insertion element was removed (solid bar). The height of each bar represents the mean of two independent RNA extractions, each then analyzed with threefold replication. Error bars are 95% confidence intervals based on the sixfold replication.

SHIBUYA and HIRAOKA 1992). Loss-of-function mutations in the *cls* gene lead to excess PG that cannot be converted to CL during stationary phase (CRONAN and VAGELOS 1972; PLUSCHKE *et al.* 1978; PLUSCHKE and OVERATH 1981). A temperature downshift causes a phase transition in a cell membrane from a fluid to a more rigid, gel-like state (HAZEL 1995). Prior research has shown that the increased PG content in *cls* mutants increases membrane fluidity, leading to a decrease of $\sim 6^\circ$ in the midpoint of this phase transition (PLUSCHKE and OVERATH 1981).

The effect of an evolved *cls* deletion mutation on membrane fluidity was tested using fluorescence anisotropy with the amphipathic probe laurdan. No single technique for characterizing membrane fluidity is sensitive to the entire range of lipid motions, and estimates of fluidity therefore depend on the motions that can be detected by particular methods (HAZEL 1995). Laurdan localizes near the phospholipid head groups in the cytoplasmic membrane and hence is useful for examining differences in membrane fluidity at the water-lipid interface. This *cls* mutation significantly increases fluidity after a FT cycle in both the evolved and the progenitor backgrounds, but it has no significant effect on fluidity during stationary phase at 37° , indicating that it helps to maintain membrane fluidity after FT stress. Freezing and thawing cause changes in hydration, and so the fact that anisotropy values differ among strains only after a FT treatment might indicate a hydration-dependent molecular rearrangement in the head-group region, as other head

groups are known to respond to changes in hydration (HSIEH *et al.* 1997).

Our findings support previous research showing that membrane fluidity plays an important role in allowing organisms to tolerate various stresses over physiological and evolutionary timescales (RAMOS *et al.* 1997; BENEY and GERVAIS 2001), including especially stresses related to temperature (MARR and INGRAHAM 1962; SINENSKY 1974; BEHAN-MARTIN *et al.* 1993; HERMAN *et al.* 1994; NEDWELL 1999). To compensate for the increased membrane rigidity caused by a temperature downshift, adaptive responses often increase membrane fluidity, a phenomenon known as “homeoviscous adaptation” (SINENSKY 1974; HAZEL 1995). The increased membrane fluidity associated with the evolved *cls* alleles, and other mutations not yet found, may promote FT survival in several ways. Disruption of the plasma membrane is the primary cause of FT injury, which leads to changes in osmotic behavior and, potentially, mechanical failure leading to cell death (STEPONKUS 1984). Membrane fluidity reduces FT injury and promotes survival during freezing and thawing in bacteria and other organisms (KRUUV *et al.* 1978; BENEY and GERVAIS 2001). We speculate that increased membrane fluidity under FTG conditions may be beneficial for a number of reasons, including improved membrane protein function (LETELLIER *et al.* 1977; CRONAN 1978; HAZEL 1995), greater membrane integrity during contractions and expansions caused by dehydration and rehydration, respectively (STEPONKUS 1984), reduced ice-crystal nucleation on the membrane surface (MINDOCK *et al.* 2001), and faster recovery of growth because DNA replication requires a fluid membrane (CASTUMA *et al.* 1993).

Physiological significance of the evolved *uspA/B* mutations: The *uspB* gene has a putative σ^S -promoter (Figure 3), and it should therefore be upregulated under various stressful conditions (FAREWELL *et al.* 1998). Yet, although UspB is named a universal stress protein, it is demonstrably beneficial for freeze-thaw survival and recovery to reduce greatly its expression. Based on its sequence, UspB is probably a membrane-associated protein, and it may be involved with maintaining membrane fluidity. However, we saw no differences in membrane fluidity, either during stationary phase or after the FT treatment, using both laurdan and DPH as probes for fluorescence anisotropy. There were also no significant differences between these strains in their ethanol sensitivity during stationary phase or after FT treatment. The physiological basis for the advantage of the *uspA/B::IS150* mutant under the FTG regime therefore remains unknown.

The fact that the *uspA/B::IS150* insertion is demonstrably beneficial under the FTG regime does not exclude the possibility that the genomic position where it inserted is a “hotspot” for this class of mutation (MAHILLON and CHANDLER 1998), although no such hotspot has been described for IS150. To search for

specific sequence motifs, we employed the MAST program (BAILEY and GRIBSKOV 1998), using 100-bp regions on either side of each *IS150* target site in *cls* and *uspA/B*. Only one potential motif was found, a 6-bp stretch (“GGGGCT”) located 4 bp downstream from the *uspA/B* target site that exactly matches an *IS150* insertion into an existing *IS1* element (HALL *et al.* 1989). A few other *IS150* insertion sites in our study are similar to this 6-bp motif, although with mismatches. Given the short length of the motif and the small number of unique *IS150* insertions in our study, its biological relevance remains unclear.

In conclusion, we found two loci, *cls* and *uspA/B*, in which several lines that had evolved under a FTG regime independently acquired mutations. Construction of and competition between isogenic strains that differ only at those loci demonstrate that the evolved alleles in both genes contribute significantly to the fitness gains under the FTG regime, including improved FT survival and faster recovery of subsequent growth. The *cls* mutation helps maintain membrane fluidity following FT treatment and contributes to increased FT survival in the evolved background. The mutations in the *uspA/B* intergenic region severely disrupt transcription of *uspB*, but the physiological basis for the resulting benefit remains unknown. Moreover, other mutations in unknown genes contribute to adaptation to the FTG regime and interact epistatically with the *cls* mutation.

We thank N. Hajela for help in the laboratory and J. Breznak, T. Schmidt, M. Thomashow, J. Tiedje, and T. Whittam for many helpful discussions and comments. This research was supported primarily by a grant from the National Aeronautics and Space Administration Astrobiology Institute to the Center for Genomic and Evolutionary Studies on Microbial Life at Low Temperature at Michigan State University, with additional support for the derivation of strains from the National Science Foundation, Université Joseph Fourier, and the Centre National de la Recherche Scientifique.

LITERATURE CITED

- ARICHA, B., I. FISHOV, Z. COHEN, N. SIKRON, S. PESAKHOV *et al.*, 2004 Differences in membrane fluidity and fatty acid composition between phenotypic variants of *Streptococcus pneumoniae*. *J. Bacteriol.* **186**: 4638–4644.
- AMES, G. F., 1968 Lipids of *Salmonella typhimurium* and *Escherichia coli*: structure and metabolism. *J. Bacteriol.* **95**: 833–843.
- BAILEY, T. L., and M. GRIBSKOV, 1998 Combining evidence using p-values: application to sequence homology searches. *Bioinformatics* **14**: 48–54.
- BEHAN-MARTIN, M. K., G. R. JONES, K. BOWLER and A. R. COSSINS, 1993 A near perfect temperature adaptation of bilayer order in vertebrate brain membranes. *Biochim. Biophys. Acta* **1151**: 216–222.
- BENEY, L., and P. GERVAIS, 2001 Influence of the fluidity of the membrane on the response of microorganisms to environmental stresses. *Appl. Microbiol. Biotechnol.* **57**: 34–42.
- BENEY, L., Y. MILLE and P. GERVAIS, 2004 Death of *Escherichia coli* during rapid and severe dehydration is related to lipid phase transition. *Appl. Microbiol. Biotechnol.* **65**: 457–464.
- BLASBAND, A. J., J. R. MARCOTTE and C. A. SCHNAITMAN, 1986 Structure of the *lc* and *nmpC* outer membrane porin protein genes of lambdaoid bacteriophage. *J. Biol. Chem.* **261**: 12723–12732.
- BONGERS, R. S., M. H. N. HOEFNAGEL, M. J. C. STARRENBURG, M. A. J. SIEMERINK, J. G. A. ARENDS *et al.*, 2003 *IS981*-mediated adaptive evolution recovers lactate production by *ldhB* transcription activation in a lactate dehydrogenase-deficient strain of *Lactococcus lactis*. *J. Bacteriol.* **185**: 4499–4507.
- BULL, J. J., M. R. BADGETT, H. A. WICHMAN, J. P. HUELSENBECK, D. M. HILLIS *et al.*, 1997 Exceptional convergent evolution in a virus. *Genetics* **147**: 1497–1507.
- CASTUMA, C. E., E. CROOKE and A. KORNBERG, 1993 Fluid membranes with acidic domains activate DnaA, the initiator protein of replication in *Escherichia coli*. *J. Biol. Chem.* **268**: 24665–24668.
- CHARLIER, D., J. PIETTE and N. GLANSORFF, 1982 *IS3* can function as a mobile promoter in *E. coli*. *Nucleic Acids Res.* **10**: 5935–5948.
- CIAMPI, M. S., M. B. SCHMID and J. R. ROTH, 1982 Transposon Tn10 provides a promoter for transcription of adjacent sequences. *Proc. Natl. Acad. Sci. USA* **79**: 5016–5020.
- COLOSIMO, P. F., K. E. HOSEMAN, S. BALABHADRA, G. VILLARREAL, JR., M. DICKSON *et al.*, 2005 Widespread parallel evolution in sticklebacks by repeated fixation of ectodysplasin alleles. *Science* **307**: 1928–1933.
- COOPER, T. F., D. E. ROZEN and R. E. LENSKI, 2003 Parallel changes in gene expression after 20,000 generations of evolution in *Escherichia coli*. *Proc. Natl. Acad. Sci. USA* **100**: 1072–1077.
- COOPER, V. S., D. SCHNEIDER, M. BLOT and R. E. LENSKI, 2001 Mechanisms causing rapid and parallel losses of ribose catabolism in evolving populations of *Escherichia coli*. *J. Bacteriol.* **183**: 2834–2841.
- CRONAN, JR., J. E., 1968 Phospholipid alterations during growth of *Escherichia coli*. *J. Bacteriol.* **95**: 2054–2061.
- CRONAN, JR., J. E., 1978 Molecular biology of bacterial membrane lipids. *Annu. Rev. Biochem.* **47**: 163–189.
- CRONAN, J. E., and P. R. VAGELOS, 1972 Metabolism and function of the membrane phospholipids of *Escherichia coli*. *Biochim. Biophys. Acta* **265**: 25–60.
- DEONIER, R. C., 1996 Native insertion sequence elements: locations, distributions, and sequence relationships, pp. 2000–2011 in *Escherichia coli and Salmonella: Cellular and Molecular Biology*, edited by F. C. NEIDHARDT. ASM Press, Washington, DC.
- DE VISSER, J. A., A. D. AKKERMANS, R. F. HOEKSTRA and W. M. DE VOS, 2004 Insertion-sequence-mediated mutations isolated during adaptation to growth and starvation in *Lactococcus lactis*. *Genetics* **168**: 1145–1157.
- DOMBEK, K. M., and L. O. INGRAM, 1984 Effects of ethanol on the *Escherichia coli* plasma membrane. *J. Bacteriol.* **157**: 233–239.
- EICHENBAUM, Z., and Z. LIVNEH, 1998 UV light induces *IS10* transposition in *Escherichia coli*. *Genetics* **149**: 1173–1181.
- ELENA, S. F., and R. E. LENSKI, 2003 Evolution experiments with microorganisms: the dynamics and genetic bases of adaptation. *Nat. Rev. Genet.* **4**: 457–469.
- FAREWELL, A., K. KVINT and T. NYSTROM, 1998 *uspB*, a new sigmaS-regulated gene in *Escherichia coli* which is required for stationary-phase resistance to ethanol. *J. Bacteriol.* **180**: 6140–6147.
- FEREA, T. L., D. BOTSTEIN, P. O. BROWN and R. F. ROSENZWEIG, 1999 Systematic changes in gene expression patterns following adaptive evolution in yeast. *Proc. Natl. Acad. Sci. USA* **96**: 9721–9726.
- HALL, B. G., 1999 Spectra of spontaneous growth-dependent and adaptive mutations at *ebgR*. *J. Bacteriol.* **181**: 1149–1155.
- HALL, B. G., L. L. PARKER, P. W. BETTS, R. F. DUBOSE, S. A. SAWYER *et al.*, 1989 *IS103*, a new insertion element in *Escherichia coli*: characterization and distribution in natural populations. *Genetics* **121**: 423–431.
- HARRIS, F. M., K. B. BEST and J. D. BELL, 2002 Use of laurdan fluorescence intensity and polarization to distinguish between changes in membrane fluidity and phospholipid order. *Biochim. Biophys. Acta* **1**: 123–128.
- HAZEL, J. R., 1995 Thermal adaptation in biological membranes: Is homeoviscous adaptation the explanation? *Annu. Rev. Physiol.* **57**: 19–42.
- HEBER, S., and B. E. TROPP, 1991 Genetic regulation of cardiolipin synthesis in *Escherichia coli*. *Biochim. Biophys. Acta* **1129**: 1–12.
- HERMAN, P., I. KONOPASEK, J. PLASEK and J. SVOBODOVA, 1994 Time-resolved polarized fluorescence studies of the temperature adaptation in *Bacillus subtilis* using DPH and TMA-DPH fluorescent probes. *Biochim. Biophys. Acta* **1190**: 1–8.

- HERRING, C. D., J. D. GLASNER and F. R. BLATTNER, 2003 Gene replacement without selection: regulated suppression of amber mutations in *Escherichia coli*. *Gene* **311**: 153–163.
- HERRING, C. D., A. RAGHUNATHAN, C. HONISCH, T. PATEL, M. K. APLEBEE *et al.*, 2006 Comparative genome sequencing of *Escherichia coli* allows observation of bacterial evolution on a laboratory timescale. *Nat. Genet.* **38**: 1406–1412.
- HIRSCHBERG, C. B., and E. P. KENNEDY, 1972 Mechanism of the enzymatic synthesis of cardiolipin in *Escherichia coli*. *Proc. Natl. Acad. Sci. USA* **69**: 648–651.
- HSIEH, C. H., S. C. SUE, P. C. LYU and W. G. WU, 1997 Membrane packing geometry of diphytanoylphosphatidylcholine is highly sensitive to hydration: phospholipids polymorphism induced by molecular rearrangement in the headgroup region. *Biophys. J.* **2**: 870–877.
- IVANISEVIC, R., M. MILIC, D. AJDIC, J. RAKONJAC and D. J. SAVIC, 1995 Nucleotide sequence, mutational analysis, transcriptional start site, and product analysis of *nov*, the gene which affects *Escherichia coli* K-12 resistance to the gyrase inhibitor novobiocin. *J. Bacteriol.* **177**: 1766–1771.
- JAURIN, B., and S. NORMARK, 1983 Insertion of IS2 creates a novel *ampC* promoter in *Escherichia coli*. *Cell* **32**: 809–816.
- JORDAN, E., H. SAEDLER and P. STARLINGER, 1968 O^o and strong polar mutations in the *gal* operon are insertions. *Mol. Gen. Genet.* **102**: 353–363.
- KRUUV, J., J. R. LEPOCK and A. D. KEITH, 1978 The effect of fluidity of membrane lipids on freeze-thaw survival of yeast. *Cryobiology* **15**: 73–79.
- KVINT, K., L. NACHIN, A. DIEZ and T. NYSTROM, 2003 The bacterial universal stress protein: function and regulation. *Curr. Opin. Microbiol.* **6**: 140–145.
- LENSKI, R. E., 2004 Phenotypic and genomic evolution during a 20,000-generation experiment with the bacterium *Escherichia coli*. *Plant Breed. Rev.* **24**: 225–265.
- LENSKI, R. E., M. R. ROSE, S. C. SIMPSON and S. C. TADLER, 1991 Long-term experimental evolution in *Escherichia coli*. I. Adaptation and divergence during 2,000 generations. *Am. Nat.* **138**: 1315–1341.
- LETELLIER, L., H. MOUDDEN and E. SHECHTER, 1977 Lipid and protein segregation in *Escherichia coli* membrane: morphological and structural study of different cytoplasmic membrane fractions. *Proc. Natl. Acad. Sci. USA* **74**: 452–456.
- MAHILLON, J., and M. CHANDLER, 1998 Insertion sequences. *Microbiol. Mol. Biol. Rev.* **62**: 725–774.
- MARR, A. G., and J. L. INGRAHAM, 1962 Effect of temperature on the composition of fatty acids in *Escherichia coli*. *J. Bacteriol.* **84**: 1260–1267.
- MINDOCK, C. A., M. A. PETROVA and R. I. HOLLINGSWORTH, 2001 Re-evaluation of osmotic effects as a general adaptive strategy for bacteria in sub-freezing conditions. *Biophys. Chem.* **89**: 13–24.
- NAAS, T., M. BLOT, W. M. FITCH and W. ARBER, 1994 Insertion sequence-related genetic rearrangements in resting *Escherichia coli* K-12. *Genetics* **136**: 721–730.
- NAAS, T., M. BLOT, W. M. FITCH and W. ARBER, 1995 Dynamics of IS-related genetic rearrangements in resting *Escherichia coli* K-12. *Mol. Biol. Evol.* **12**: 198–207.
- NEDWELL, D. B., 1999 Effect of low temperature on microbial growth: lowered affinity for substrates limits growth at low temperature. *FEMS Microbiol. Ecol.* **30**: 101–111.
- OHTSUBO, Y., H. GENKA, H. KOMATSU, Y. NAGATA and M. TSUDA, 2005 High-temperature-induced transposition of insertion elements in *Burkholderia multivorans* ATCC 17616. *Appl. Environ. Microbiol.* **71**: 1822–1828.
- PAPADOPOULOS, D., D. SCHNEIDER, J. MEIER-EISS, W. ARBER, R. E. LENSKI *et al.*, 1999 Genomic evolution during a 10,000-generation experiment with bacteria. *Proc. Natl. Acad. Sci. USA* **96**: 3807–3812.
- PELOSI, L., L. KÜHN, D. GUETTA, J. GARIN, J. GEISELMANN *et al.*, 2006 Parallel changes in global protein profiles during long-term experimental evolution in *Escherichia coli*. *Genetics* **173**: 1851–1869.
- PLUSCHKE, G., and P. OVERATH, 1981 Function of phospholipids in *Escherichia coli*. Influence of changes in polar head group composition on the lipid phase transition and characterization of a mutant containing only saturated phospholipid acyl chains. *J. Biol. Chem.* **256**: 3207–3212.
- PLUSCHKE, G., Y. HIROTA and P. OVERATH, 1978 Function of phospholipids in *Escherichia coli*. Characterization of a mutant deficient in cardiolipin synthesis. *J. Biol. Chem.* **253**: 5048–5055.
- POON, A., and L. CHAO, 2005 The rate of compensatory mutation in the DNA bacteriophage phiX174. *Genetics* **170**: 989–999.
- RAMOS, J. L., E. DUQUE, J. J. RODRIGUEZ-HERVA, P. GODOY, A. HAIDOUR *et al.*, 1997 Mechanisms for solvent tolerance in bacteria. *J. Biol. Chem.* **272**: 3887–3890.
- REIF, H. J., and H. SAEDLER, 1975 IS1 is involved in deletion formation in the *gal* region of *E. coli* K12. *Mol. Gen. Genet.* **137**: 17–28.
- REYNOLDS, A. E., J. FELTON and A. WRIGHT, 1981 Insertion of DNA activates the cryptic *bgl* operon in *Escherichia coli* K12. *Nature* **293**: 625–629.
- RIEHLE, M. M., A. F. BENNETT and A. D. LONG, 2001 Genetic architecture of thermal adaptation in *Escherichia coli*. *Proc. Natl. Acad. Sci. USA* **98**: 525–530.
- RIEHLE, M. M., A. F. BENNETT and A. D. LONG, 2005 Changes in gene expression following high-temperature adaptation in experimentally evolved populations of *E. coli*. *Physiol. Biochem. Zool.* **78**: 299–315.
- RILEY, M., T. ABE, M. B. ARNAUD, M. K. BERLYN, F. R. BLATTNER *et al.*, 2006 *Escherichia coli* K-12: a cooperatively developed annotation snapshot—2005. *Nucleic Acids Res.* **34**: 1–9.
- SANGER, F., S. NICKLEN and A. R. COULSON, 1977 DNA sequencing with chain-terminating inhibitors. *Proc. Natl. Acad. Sci. USA* **74**: 5463–5467.
- SCHNEIDER, D., and R. E. LENSKI, 2004 Dynamics of insertion sequence elements during experimental evolution of bacteria. *Res. Microbiol.* **155**: 319–327.
- SCHNEIDER, D., E. DUPERCHY, E. COURSANGE, R. E. LENSKI and M. BLOT, 2000 Long-term experimental evolution in *Escherichia coli*. IX. Characterization of insertion sequence-mediated mutations and rearrangements. *Genetics* **156**: 477–488.
- SCHNEIDER, D., E. DUPERCHY, J. DEPEYROT, E. COURSANGE, R. E. LENSKI *et al.*, 2002 Genomic comparisons among *Escherichia coli* strains B, K-12, and O157:H7 using IS elements as molecular markers. *BMC Microbiol.* **2**: 18.
- SCHOUSTRA, S. E., A. J. DEBETS, M. SLAKHORST and R. F. HOEKSTRA, 2006 Reducing the cost of resistance: experimental evolution in the filamentous fungus *Aspergillus nidulans*. *J. Evol. Biol.* **19**: 1115–1127.
- SCHWARTZ, E., M. KROGER and B. RAK, 1988 IS150: distribution, nucleotide sequence and phylogenetic relationships of a new *E. coli* insertion element. *Nucleic Acids Res.* **16**: 6789–6802.
- SHIBUYA, I., and S. HIRAOKA, 1992 Cardiolipin synthase from *Escherichia coli*. *Methods Enzymol.* **209**: 321–330.
- SINENSKY, M., 1974 Homeoviscous adaptation—a homeostatic process that regulates the viscosity of membrane lipids in *Escherichia coli*. *Proc. Natl. Acad. Sci. USA* **71**: 522–525.
- SLEIGHT, S. C., 2007 Survival and experimental evolution of *Escherichia coli* under freeze-thaw stress. Ph.D. Dissertation, Michigan State University, East Lansing, MI.
- SLEIGHT, S. C., and R. E. LENSKI, 2007 Evolutionary adaptation to freeze-thaw-growth cycles in *Escherichia coli*. *Phys. Biochem. Zool.* **80**: 370–385.
- SLEIGHT, S. C., N. S. WIGGINTON and R. E. LENSKI, 2006 Increased susceptibility to repeated freeze-thaw cycles in *Escherichia coli* following long-term evolution in a benign environment. *BMC Evol. Biol.* **6**: 104.
- SOUTHERN, E. M., 1975 Detection of specific sequences among DNA fragments separated by gel electrophoresis. *J. Biol. Chem.* **98**: 503–517.
- STEPONKUS, P. L., 1984 Role of the plasma membrane in freezing injury and cold acclimation. *Annu. Rev. Plant Physiol.* **35**: 543–584.
- TREVES, D. S., S. MANNING and J. ADAMS, 1998 Repeated evolution of an acetate-crossfeeding polymorphism in long-term populations of *Escherichia coli*. *Mol. Biol. Evol.* **15**: 789–797.
- TWISS, E., A. M. COROS, N. P. TAVAKOLI and K. M. DERBYSHIRE, 2005 Transposition is modulated by a diverse set of host factors in *Escherichia coli* and is stimulated by nutritional stress. *Mol. Microbiol.* **57**: 1593–1607.

- VANOUNOU, S., D. PINES, E. PINES, A. H. PAROLA and I. FISHOV, 2002 Coexistence of domains with distinct order and polarity in fluid bacterial membranes. *Photochem. Photobiol.* **76**: 1–11.
- VELICER, G. J., G. RADDATZ, H. KELLER, S. DEISS, C. LANZ *et al.*, 2006 Comprehensive mutation identification in an evolved bacterial cooperator and its cheating ancestor. *Proc. Natl. Acad. Sci. USA* **103**: 8107–8112.
- WICHMAN, H. A., M. R. BADGETT, L. A. SCOTT, C. M. BOULIANNE and J. J. BULL, 1999 Different trajectories of parallel evolution during viral adaptation. *Science* **285**: 422–424.
- WOOD, T. E., J. M. BURKE and L. H. RIESEBERG, 2005 Parallel genotypic adaptation: when evolution repeats itself. *Genetica* **123**: 157–170.
- WOODS, R., D. SCHNEIDER, C. L. WINKWORTH, M. A. RILEY and R. E. LENSKI, 2006 Tests of parallel molecular evolution in a long-term experiment with *Escherichia coli*. *Proc. Natl. Acad. Sci. USA* **103**: 9107–9112.
- ZINSER, E. R., D. SCHNEIDER, M. BLOT and R. KOLTER, 2003 Bacterial evolution through the selective loss of beneficial genes: trade-offs in expression involving two loci. *Genetics* **164**: 1271–1277.

Communicating editor: J. LAWRENCE